

Heterodyne swept-source optical coherence tomography for complete complex conjugate ambiguity removal

Anjul Maheshwari, Michael A. Choma, Joseph A. Izatt
Department of Biomedical Engineering, Duke University, Durham, NC USA 27708

ABSTRACT

Fourier domain techniques have increasingly gained attention in the optical coherence tomography field. This is mainly due to demonstrated sensitivities of two to three orders of magnitude greater than conventional time domain techniques. FDOCT images are plagued with two sources of ambiguity and artifact. First, complex conjugate ambiguity arises from the Fourier transform of the real-valued interferometric signal. This ambiguity causes a superposition of reflectors at positive and negative pathlength differences between the sample and reference reflectors. Secondly, the source spectral shape and sample autocorrelation terms appear at DC, thereby obscuring reflectors at zero pathlength difference. In this paper, we show that heterodyne detection in swept-source OCT (SSOCT) allows for the resolution of complex conjugate ambiguity and the removal of spectral and autocorrelation artifacts. We show that frequency shifting of the reference arm optical field, by use of acousto-optic modulators, upshifts the cross-interferometric signal to a user-tunable electronic frequency that corresponds to an adjustable electronic pathlength mismatch between the interferometer arms. This electronic pathlength mismatching recenters the A-scan at an offset that can be far from DC, which effectively resolves the complex conjugate ambiguity problem. Additionally, spectral and autocorrelation terms still reside near DC, which allows them to be removed by high-pass filtering. We also show that complex conjugate ambiguity resolution via frequency shifting is immune to falloff induced by finite source linewidth in SSOCT.

Keywords: optical coherence tomography, Fourier-domain, heterodyne, complex conjugate ambiguity removal

1. INTRODUCTION

Fourier domain optical coherence tomography (FDOCT) techniques have reshaped the OCT landscape due to demonstrated sensitivities that are two to three orders of magnitude greater than their time domain counterparts. This sensitivity advantage has been confirmed both theoretically and experimentally.¹⁻³ The primary features of FDOCT systems are that they feature line rates in the tens of kilohertz regime with sensitivities comparable to previous state-of-the-art time domain systems.

The shift to FDOCT, however, is not without costs. FDOCT images contain two important sources of ambiguity and artifact. First, since the Fourier transform of a real-valued Fourier domain interferometric signal is Hermitian symmetric, sample reflectors at a positive displacement, $+\Delta x$, with respect to the reference reflector, are superimposed on those at a negative displacement, $-\Delta x$. Second, the source spectral shape and sample autocorrelation terms transform to $\Delta x = 0$, thereby obscuring reflectors positioned at zero pathlength difference. These artifacts can be removed by retrieval of the complex interferometric signal.

Previous techniques for collecting the complex Fourier domain interferometric signal have relied on collecting the in-phase and $\pi/2$ -shifted (quadrature) components generated by phase stepping interferometry⁴ or by 3x3 interferometry.^{5,6} These techniques are constrained to homodyne insofar as both the reference and sample arm optical fields have the same phase velocity. Homodyne detection is required for spectral-domain OCT (SDOCT) systems that employ spectrometers coupled to charge accumulation detectors such as charge-coupled devices (CCDs) and photodiode arrays. In swept-source OCT, however, a current-generating photodiode is employed, which allows the spectral interferometric signal to be encoded with a characteristic heterodyne beat frequency.

In this paper we show that heterodyne detection in swept-source OCT (SSOCT) allows for the resolution of complex conjugate ambiguity and the removal of spectral and autocorrelation artifact. We show that frequency shifting of the reference arm optical field upshifts the cross-interferometric signal to a user-tunable frequency that corresponds to an electronic pathlength mismatch between the interferometer arms. This electronic pathlength mismatching recenters the A-scan at an offset that can be far from DC, which effectively resolves the complex conjugate ambiguity problem.

Additionally, spectral and autocorrelation terms still reside near DC, which allows them to be removed by high-pass filtering. While it is also possible, in principle, to upshift the cross-interferometric signal by placing the sample focus at a large pathlength mismatch, this physical pathlength mismatching leads to significant signal attenuation due to amplitude falloff secondary to finite source linewidths.^{4,5} We also show that complex conjugate ambiguity resolution via frequency shifting is immune to this falloff phenomenon.

2. THEORETICAL ANALYSIS

2.1 Imaging Depth

The imaging depth achieved using FDOCT systems is described in two ways; the maximum imaging depth and falloff. The maximum imaging depth in FDOCT systems is related to² :

$$\Delta z_{\max} = \frac{1}{4d_s k} \quad (1)$$

where Δz_{\max} is the maximum imaging depth where aliasing causes signals from deeper reflectors to fold onto itself. δk is defined as the spectral sampling interval of the FDOCT system. In SDOCT systems, the spectral sampling interval is limited by the pixel spacing of the CCD. For SSOCT systems, the spectral sampling interval is only limited by the sampling rate of the analog-digital acquisition board.

The second parameter that determines the imaging depth of FDOCT systems is falloff. Falloff is caused by fringe washout and it describes the SNR degradation as a function of imaging depth. The -3dB falloff point which was derived from falloff analysis reported by Yun, et., al.⁷ is given by:

$$\Delta z_{-3dB} = \frac{2 \ln 2}{d_r k} \quad (2)$$

where Δz_{-3dB} is the imaging depth at which the SNR is reduced by half. δk is the spectral resolution of the FDOCT system. In SDOCT, the spectral resolution is limited by the spectrometer optics and/or the pixel width of the CCD. For SSOCT systems, the spectral resolution is defined by the instantaneous linewidth of the swept laser source. Swept laser sources with linewidths smaller than the resolution of SDOCT spectrometers are readily available and therefore give SSOCT an over two-fold imaging depth advantage over SDOCT techniques. Imaging depth capabilities over 4mm can be valuable for applications such as endoscopy, small animal imaging, and human anterior segment imaging.

2.2 Heterodyne SSOCT

In FDOCT, the photocurrent signal generated by n reflectors is related to

$$i(k) \propto S(k) \left[R_R + \sum_n R_n + 2\sqrt{R_R} \sum_n \sqrt{R_n} \cos(2k[z_R - z_n]) + 2 \sum_n \sum_{m \neq n} \sqrt{R_n R_m} \cos(2k[z_n - z_m]) \right] \quad (3)$$

Here, $i(k)$ is the detector photocurrent as a function of optical wavenumber k ; $S(k)$ is the source power spectral density; R_R and R_n are the reflectivities of the reference and n^{th} sample reflector, respectively; and z_R and z_n are the positions of the reference and n^{th} sample reflector, respectively. The first two terms in the brackets on the right-hand side represents non-interferometric spectral artifact. The third term represents the cross-interferometric terms, and the fourth term represents the autocorrelation artifact.

Wavenumber is parameterized by time t by the relationship $k=k_o+t(dk/dt)$, where k_o is the starting wavenumber and dk/dt is the sweep velocity. This sweeping leads to the conversion of pathlength differences in the auto- and cross-terms to an electronic beat frequency in $i(t)$, the time-varying photocurrent. The cross frequencies have instantaneous values of $\mathbf{w}_n=(dk/dt)[z_R - z_n]$, while the auto frequencies have instantaneous values of $\mathbf{w}_{nm}=(dk/dt)[z_n - z_m]$. If the reference arm optical field is shifted by some frequency \mathbf{w}_D , then the time-varying photocurrent becomes:

$$i(t) \propto S(t) \left[R_R + \sum_n R_n + 2\sqrt{R_R} \sum_n \sqrt{R_n} \cos([\mathbf{w}_n + \mathbf{w}_D]t + \mathbf{f}_n) + 2 \sum_n \sum_{m \neq n} \sqrt{R_n R_m} \cos(\mathbf{w}_{nm}t + \mathbf{f}_{nm}) \right] \quad (4)$$

where $\mathbf{f}_n=k_o[z_n-z_m]$ and $\mathbf{f}_{nm}=k_o[z_n-z_m]$. After frequency shifting, the autocorrelation and source spectral terms remain centered at baseband, while the cross-interference terms are recentered around \mathbf{w}_D . While the Fourier transform of $i(t)$ remains Hermitian symmetric, the transform of fringes generated by pathlength differences of equal magnitude but opposite sign no longer overlap. This resolves complex conjugate ambiguity because positive displacements are above

w_D , while negative displacements are below w_D as long as w_D is larger than the maximum w_n . If the wavenumber sweep is linear over a bandwidth sweep Δk that takes Δt seconds to complete, then w_D corresponds to a pathlength shift of $z_D = w_D \Delta t / (2\Delta k)$. This shift does not lead to signal falloff. Falloff in SSOCT occurs because the interferometric signal is integrated over the source linewidth at the photodiode. If the source linewidth is on the order of $2\pi / (z_R - z_n)$, then the linewidth spans an appreciable portion of the interferometric fringe. This decreases the fringe visibility, which decreases the peak height in the Fourier transform of $i(t)$. Frequency shifting creates a time-varying beat frequency that is independent of sweep speed or source linewidth and, as such, it is not susceptible to falloff.

The cross-interferometric signal can be recovered by band pass filtering around w_D with a noise equivalent bandwidth of $NEB = 2z_{max} \Delta k / \Delta t$. If demodulation is performed, the band-passed signal is mixed with orthogonal local oscillators with frequency w_D , then the real and imaginary parts of the complex interferometric signal can be recovered:

$$\begin{aligned} i_{re}(t) &= 2S(t) \sqrt{R_R} \sum \sqrt{R_n} \cos(w_n t + f_n) \\ i_{im}(t) &= 2S(t) \sqrt{R_R} \sum \sqrt{R_n} \sin(w_n t + f_n) \end{aligned} \quad (5)$$

Additionally, demodulation enables wavenumber triggering^{8,9} of the above interferometric signals, thereby eliminating the need to resample the data in software.

Finally, it should be noted that an analogous technique for complex conjugate ambiguity removal could be implemented in SDOCT by use of spatial heterodyning and demodulation techniques.

3. EXPERIMENTAL SETUP

We constructed the heterodyne SSOCT setup shown in Fig. 1 using a fiber-based swept laser source (Micron Optics, Inc. $\lambda_0 = 1310\text{nm}$, $\Delta\lambda = 100\text{nm}$, 250Hz sweep rate), acousto-optic modulators (IntraAction, Corp.), and a New Focus balanced photodetector. The acousto-optic modulators (AOs) had a common center frequency of 100MHz, one having a user-adjustable offset from that frequency. The diffraction efficiency of the AOs was measured to be 60%, and using the simple optical setup depicted in the figure, the maximum diffracted optical bandwidth recoupled was 64nm. Spectral interferogram samples evenly spaced in wavenumber were clocked into the data acquisition system by using a fiber Fabry-Perot interferometer. The heterodyne interferometric signal is high-pass filtered to remove the spectral and auto-correlation artifacts then demodulated by mixing with a local oscillator (LO) of frequency ω_d . The inphase and quadrature components are lowpass filtered and digitized. The output power of the swept-laser source was 500 μW . There was approximately -6dB source power attenuation in the system prior to the sample, resulting in 50 μW illumination on the sample (cornea). The SNR of the system, near zero pathlength difference, with a -60dB reflector, was measured to be 99dB. The predicted SNR was 112dB. Note, the power on the eye is significantly lower than allowable, therefore the SNR of the system could be greatly increased by use of a higher power laser source.

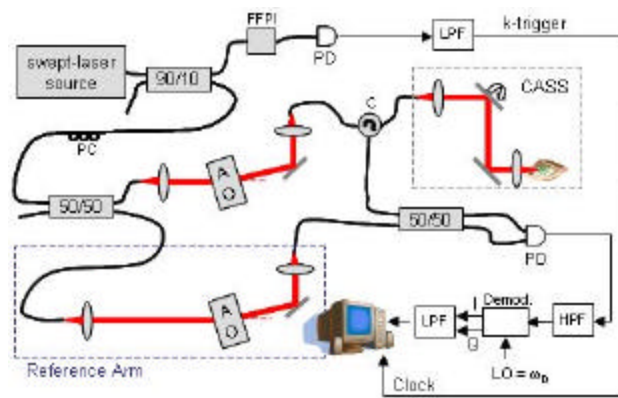


Figure 1. Heterodyne swept-source OCT system utilizing acousto-optic modulators. The swept-laser source has a center wavelength $\lambda_0 = 1310\text{nm}$ and bandwidth $\Delta\lambda = 100\text{nm}$. A balanced detector is used for DC artifact suppression. FFPI: fiber Fabry-Perot interferometer; PC: polarization controllers; AO: acousto-optic modulator; C: circulator; CASS: anterior segment scanner.

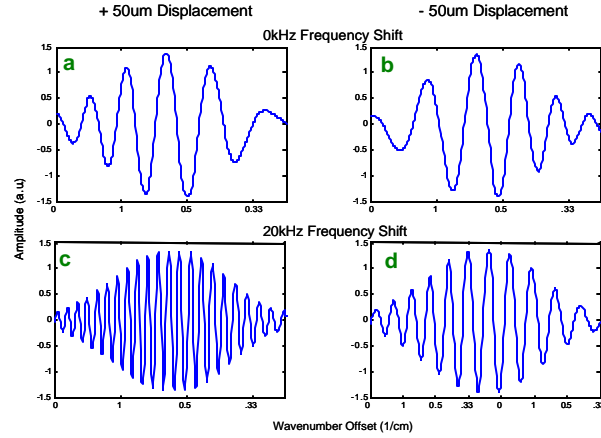


Figure 2. Interferograms taken using heterodyne SSOCT. (a) and (b) are taken from a reflector at +50 μm and -50 μm pathlength difference, respectively with a 0kHz frequency shift. (c) and (d) are collected at the same pathlength difference, but with a 20kHz frequency shift. By using heterodyne detection, reflectors at positive positions produce higher fringe frequencies than those at negative positions and therefore are unambiguously resolved.

4. RESULTS

To illustrate the behavior of the cross-interferometric term in Eq. 3 with the reference arm frequency shifted with respect to the sample arm, we show in Fig. 2 the fringe patterns of typical interferograms at two pathlength differences, centered around zero, with no frequency shift (Fig 2(a) and 2(b)), and with 20kHz frequency shift (Fig 2(c) and 2(d)). The fringe frequency for the cross-correlation term, when $w_D = 0$, is identical for positive and negative equal displacements, and is thus ambiguous. However, when $w_D = 20\text{kHz}$, the fringe frequency for the positive displacement is higher than for a negative displacement, as expected from Eq. 4.

Figure 3 illustrates that the signal falloff remains centered at zero pathlength difference, even as the electronic frequency is shifted. Figure 3(a) shows falloff centered at zero pathlength and zero frequency for homodyne SSOCT. By shifting the zero pathlength difference frequency to 1MHz (Fig. 3(b)), the image contents are moved away from DC and therefore removal of DC and auto-correlation artifacts is achieved. In Fig. 4, removal of complex conjugate ambiguity and DC artifacts is demonstrated using heterodyne SSOCT. Using a -50dB sample reflector placed at 2.0mm pathlength difference, the complex conjugate ambiguity is clearly shown in the A-scan acquired using homodyne SSOCT (Fig 4(a)). Residual DC artifact is also present in the A-scan. By upshifting the frequency of the reference arm by 140kHz, the complex conjugate ambiguity is completely resolved down to the noise floor of the system (Fig. 4(b)). In Fig. 4(b), the reflections located near zero pathlength difference originates from a neutral density filter. *In vivo* images acquired using homodyne and heterodyne SSOCT techniques are shown in Fig. 5(a) and 5(b), respectively.

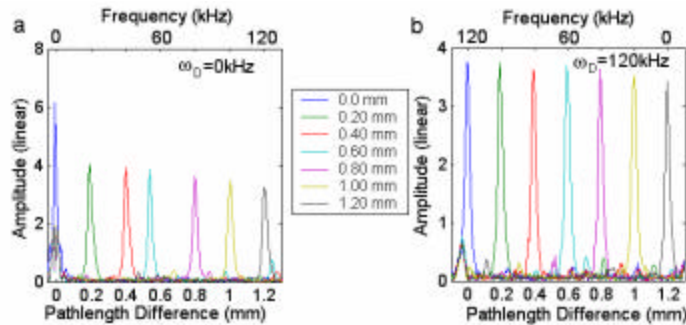


Figure 3. Falloff measurements for (a) homodyne and (b) heterodyne SSOCT. Heterodyne SSOCT enables frequency shifting of zero pathlength difference away from DC and auto-correlation artifacts, while falloff stays centered around zero pathlength difference. -50 dB reflector used in sample arm.

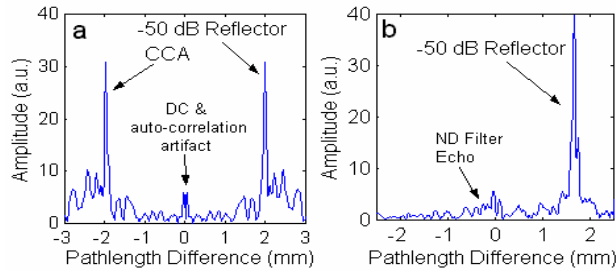


Figure 4. A-scans of a -50dB reflector at 2.0mm pathlength difference. (a) A-scan showing unresolvable complex conjugate ambiguity (CCA) acquired using homodyne SSOCT. The CCA prevents distinguishing reflectors at $+2.0\text{mm}$ from those at -2.0mm depth. Using heterodyne SSOCT (b), the CCA is resolved down to the noise floor of the system. The echo is a double-pass reflection from the ND filter, and shifts with the main reflector peak.

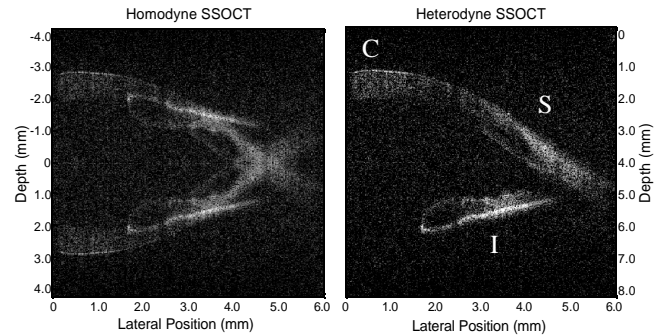


Figure 5. *In vivo* images of human anterior segment using (a) homodyne and (b) heterodyne SSOCT techniques. Complete complex conjugate ambiguity removal and doubling of the imaging depth is shown to be necessary in order to visualize the entire anterior segment of the eye. C: cornea; S: sclera; I: iris.

These images are of the anterior segment of a human eye and were acquired at a rate of 250 Hz . In the homodyne SSOCT image the iris, cornea, and sclera are hidden by the mirror image that arises from the complex conjugate artifact. Using heterodyne SSOCT, however, the artifact is completely removed and the cornea, iris, and sclera are no longer obscured. It is also clear that at least 6mm imaging depth is necessary to visualize the entire anterior segment.

5. CONCLUSIONS

In summary, we have demonstrated heterodyne SSOCT using acousto-optic modulators for complex conjugate ambiguity and DC artifact removal. This technique allows for zero pathlength difference to be shifted away from electronic DC with no penalty due to finite laser linewidth falloff. Combined with coherent demodulation, this technique provides access to the entire complex interferometric signal as well as enables wavenumber triggering, hereby eliminating the need for resampling the data in software. We have shown that this technique is essential for human anterior segment imaging applications where more than 6mm imaging depth is necessary.

ACKNOWLEDGEMENTS

We gratefully acknowledge support for this work through a grant from the National Institute of Health, R21 EB000243.

REFERENCES

1. Leitgeb, et. al., *Opt. Exp.* **11**(8), 889-894 (2003).
2. Choma, et. al., *Opt. Exp.* **11**(18), 2183-2189 (2003).
3. de Boer, et. al., *Opt. Lett.* **28**(21), 2067-2069 (2003).
4. Wojtkowski, et. al., *Opt. Lett.* **27**(16), 1415-1417 (2002).
5. Choma, et. al., *Opt. Lett.* **28**(22), 2162-2164 (2003).
6. Sarunic, et. al., *Proceedings of SPIE*, San Jose, CA (2004).
7. Yun, et. al., *Opt. Exp.*, **11**(26), 3598-3604 (2003).
8. Choma, et. al., *Proceedings of SPIE*, San Jose, CA (2004).
9. Choma, et. al., *J. Biomed. Opt.*, in press.